



Effect of High-Velocity Oxy-Fuel (HVOF) sprayed Tungsten Carbide Nickel (WC-Ni) Coating on the Fatigue Strength of Carbon Steel with Different Spraying Distances

Muhammad Nabil Fikri Norulhelmi¹, Mohd Azhar Harimon^{1,*}, Mohammad Sukri Mustapa¹, Nafisah Arina Hidayati²

¹ Department of Mechanical Engineering, Faculty of Mechanical and Manufacturing Engineering, Universiti Tun Hussein Onn Malaysia, 86400 Batu Pahat, Johor, Malaysia

² Department of Mechanical Engineering, Faculty of Engineering, Brawijaya University, Malang, Indonesia

ARTICLE INFO

Article history:

Received 17 March 2024

Received in revised form 12 May 2024

Accepted 26 May 2024

Available online 30 June 2024

Keywords:

Carbon steel; WC-Ni coating; fatigue; HVOF; spray distance

ABSTRACT

This research aims to determine the impact of varied spraying distances of 200 and 250 mm for HVOF spraying of tungsten carbide-nickel (WC-Ni) coating on the fatigue strength of S50C carbon steel. The fatigue test is performed on the coated specimens using the Shimadzu Servopulsor testing machine according to ASTM E466 for axial fatigue testing. The fracture surface was analysed by scanning electron microscope (SEM). The findings showed that the fatigue strength of the coated carbon steel decreased compared to the uncoated specimen. Also, the coated carbon steel fatigue strength increased with increasing spraying distances from 200 mm to 250 mm. There are two separate zones on the shattered surface: a burnished, smooth region and a granular, rough region. The fatigue fracture developed in the area that was burnished and smooth.

1. Introduction

The high-velocity oxy-fuel (HVOF) is referred to as thermal spray coating. It is a technique to enhance the surface quality or repair damaged components [1]. A fluid fuel and oxygen mixture is introduced into a combustion chamber and ignited to achieve the desired coating effect. It is often used in depositing cobalt-based, nickel-based, and iron-based coatings on metal substrates [2]. HVOF sprayed coating offers advantages such as enhanced cohesive strength of the coating and improved adhesion to the underlying substrate. The process of HVOF is gases flow through the nozzle at rates greater than the speed of sound due to the pressure and temperature created by gas burning. Nozzles in the combustion chamber oversee melting powder pieces completely or particularly [3].

With outstanding corrosion resistance and high-temperature tolerance, tungsten carbide-nickel (WC-Ni) is commonly employed in thermal surfacing techniques. The WC-Ni coating is particularly

* Corresponding author.

E-mail address: mazhar@uthm.edu.my

suitable for severe wear conditions due to its remarkable thickness, and abrasive media, where it exhibits greater ductility compared to tungsten carbide cobalt coating, resulting in enhanced chip resistance [4]. Additionally, it has been shown that the rate of wear of pure abrasion tungsten carbide boosts the already significant amount of carbide corrosion present throughout the sedimentation process [5]. Also, some researchers stated that the nickel may be combined with other materials to coat or protect them from the effects of corrosion [6].

Unlike other steel types, carbon steel lacks chromium, making it more prone to rust and corrosion [7]. Prolonged exposure to moisture leads to rust formation. A coating is applied to safeguard the surface of carbon steel and prevent rust. Surface coating is a practical way to add desirable qualities to materials, equipment, and machine parts, such as resistance to corrosion, erosion, and wear [8]. The coating process involved the utilisation of thermal spray in a non-metallic environment. The higher precipitate strengthening may account for the lower yield stress's proportionate influence on grain boundary strengthening [9].

Fatigue properties play a crucial role in materials' mechanical behaviour, and sufficient fatigue resistance is essential for the practical use of structural materials. Fatigue resistance refers to the ability of a material to withstand cyclic stress without accumulating damage that could result in fracture [10]. This condition eventually leads to fracture. Metal fatigue can cause unforeseen and potentially catastrophic failures in components that experience repetitive loading or stress. It is the primary cause of structural component failures in various applications such as aircraft, spacecraft, bridges, and power plants.

Previous research M.P Nascimento's study investigated the long-term impact of HVOF coating on the fatigue characteristics of carbon steel. The research focused on analysing the fatigue, abrasion, and corrosion behaviour of AISI 4340 high-strength steel, specifically concerning tungsten carbide thermal spray coating applied through HVOF and hard Cr electroplating methods [4]. Although the technique induced compressive residual stresses, the presence of a high density of pores and oxide inclusions within the coating, commonly observed during the thermal spray process, may have counteracted its benefits. Fatigue failures usually start at the surface of a fatigue specimen. In the case of coated components, the crack can initiate from the coating at the locations of pores in the coating. Once initiated, crack propagation will occur, leading to fatigue failure [3]. Also, based on Halmi's study [11], a detailed fracture surface analysis showed two noticeable regions: the burnished and granular zones. As the stress amplitude increased, there was a decrease in the size of the burnished area, indicating a reduction in the cross-sectional area of the fatigue fracture zone.

Distance from the object being sprayed has a major impact on the effectiveness of the thermal spray method. The spraying distance has been shown to influence the deposition deficit in cold spraying. The effectiveness of the deposition decreases in proportion to the increasing spraying distance [12]. The specimen's fracture toughness will decrease as the spray distance rises; however, there is no direct correlation between the spray distance and the elastic modulus or the Poisson's ratio of the specimen [13]. The number of non-melted surface roughness particles, holes and fissures between the lamellas, and the quality of the thermal spray coatings put down in the current experiment are all negatively impacted by increasing spray distance [14]. For example, when considering porosity, the fuel flow rate is the most important spraying element to consider [15].

This research investigated the effects of the HVOF process of carbon steel coated with tungsten carbide nickel on fatigue behaviour at different spraying distances. The fatigue test is conducted to assess the fatigue strength of a material when exposed to repeated cyclic loading.

2. Methodology

In this study, the specimen's substrate is made using S50C hot rolled medium carbon steel. Meanwhile, the coating is made of tungsten carbide-nickel (WC-Ni) powder. Particle size distribution of 30 to 60 μm was used. Table 1 shows the composition of S50C carbon steel and WC-Ni powder.

Table 1
 Composition of carbon steel and WC-Ni powder

Types	Weight (%)	
Carbon Steel	Fe	Balance
	C	0.52
	Si	0.27
	Mn	0.64
	P	0.016
	S	0.004
WC-Ni Powder	W	Balance
	Ni	10.21
	C	5.17
	Fe	0.68

The S50C carbon steel specimen underwent CNC milling to achieve a particular specimen's dimensions. To conduct the fatigue test, the carbon steel specimen was shaped into a dog bone configuration, as shown in Figure 1, following the guidelines of ASTM E466 [16]. The dog bone-shaped specimens have a gauge size of 6 millimetres and a gauge length of 31.06 millimetres.

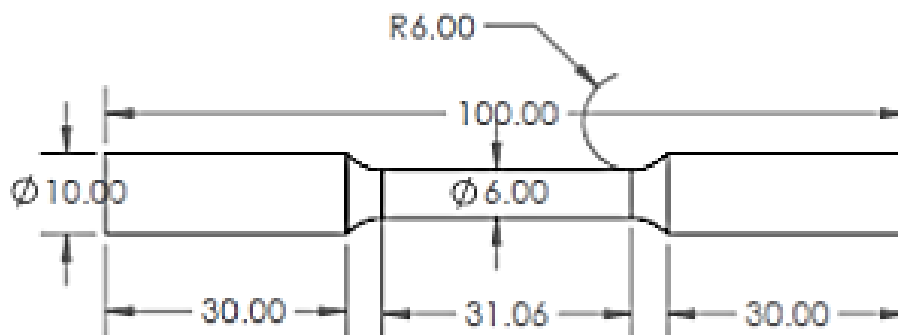


Fig. 1. Dog bone shape specimen for fatigue test

Before the HVOF process takes place, a few preparations of the substrate need to be done to attain an optimum coating. Initially, the specimens were cleaned with acetone to remove dirt, mill, and rust scale. Then, the substrate was grit-blasted using Shipblast 600 Lbs. Aluminium silicate, Al_2SiO_5 , with a 20 - 40 mesh size, was used as the abrasive material. The airflow pressure was set at 8 bar, the standoff distance between the torch and substrate was set at 100 mm, and the blowing pressure angle was kept at 90° . The outcome surface roughness of the specimen was in the range of $R_a = 1.9 - 3.2 \mu\text{m}$.

The Bexxon ZB-2000 Mobile HVOF system, equipped with the Diamond Jet DJ2700 gun, was utilised to achieve high-speed spraying of the HVOF coating powder. This process aimed to generate a dense and hard coating. The powder underwent preheating to optimise the coating's performance, facilitating chemical reactions and polymerisation among its constituents. In the case of a dog-bone-shaped specimen, the coating was applied to cover the central section. Consistency was maintained

across all specimens by keeping the coating parameters constant, as outlined in Table 2. The surface morphology of the coatings was observed using the scanning electron microscope (SEM).

Table 2
Coating parameters [11]

Parameter	Value
Thermal Spray Gun	Diamond Jet DJ2700 of Bexxon
Powder Feeding Rate	15-150 g/min
Particle Size	45 ± 15 µm
Oxygen Pressure	1.2 MPa
Fuel Pressure	0.62 MPa
Air Pressure	0.72 MPa
Air Flow	440 L/min
Fuel Flux	88 L/min
Oxygen Flux	310 L/min
Spraying Distance (mm)	200, 250

This study employed an axial fatigue test following the load-controlled approach with a load ratio (R) of -1. The cyclic loading was applied tension-compression using a sine wave pattern, conforming to the specifications outlined in ASTM E466 [16]. A load frequency of 20 Hz was selected to establish the test conditions. This frequency determines the rate at which the cyclic loads are applied to the material during the test. Additionally, a predetermined cycle count of 10^6 cycles was chosen as the target for the test. This cycle count signifies the complete load cycles the material undergoes during testing. By conducting the fatigue test according to these standardised parameters, the researchers aimed to evaluate and determine the fatigue strength of the material under consideration. The test design and adherence to established standards ensure consistency and comparability of results for accurate assessment and characterisation of the material's fatigue behaviour. After finishing the fatigue testing for the specimen, the fractured surface of the specimen of carbon steel coated with WC-Ni was observed using SEM to analyse the features of the fractured surface.

3. Results

3.1 Coating Surface Morphology

The surface morphology of the WC-Ni coatings is shown in Figure 2. The distribution of tungsten carbide (WC) consists of an angular shape, which is in light contrast and dissolves into a metallic binder of Ni, which is in dark contrast. Pores have been observed on the top surface of the coating. The resulting coatings are made up of continuous splats of thermal spraying. Pores were formed due to the random build-up, curling up and incomplete filling of splats' interstices during the thermal spray process [17]. Generally, it can be observed that the porosity of the coating for a 250 mm spraying distance increases literally if compared with the coating for a 200 mm spraying distance. A study [1] sprayed stainless steel powder using the HVOF technique, and they reported the same observations where short and moderate spray distances reduce the porosity of the coating and improve its mechanical properties.

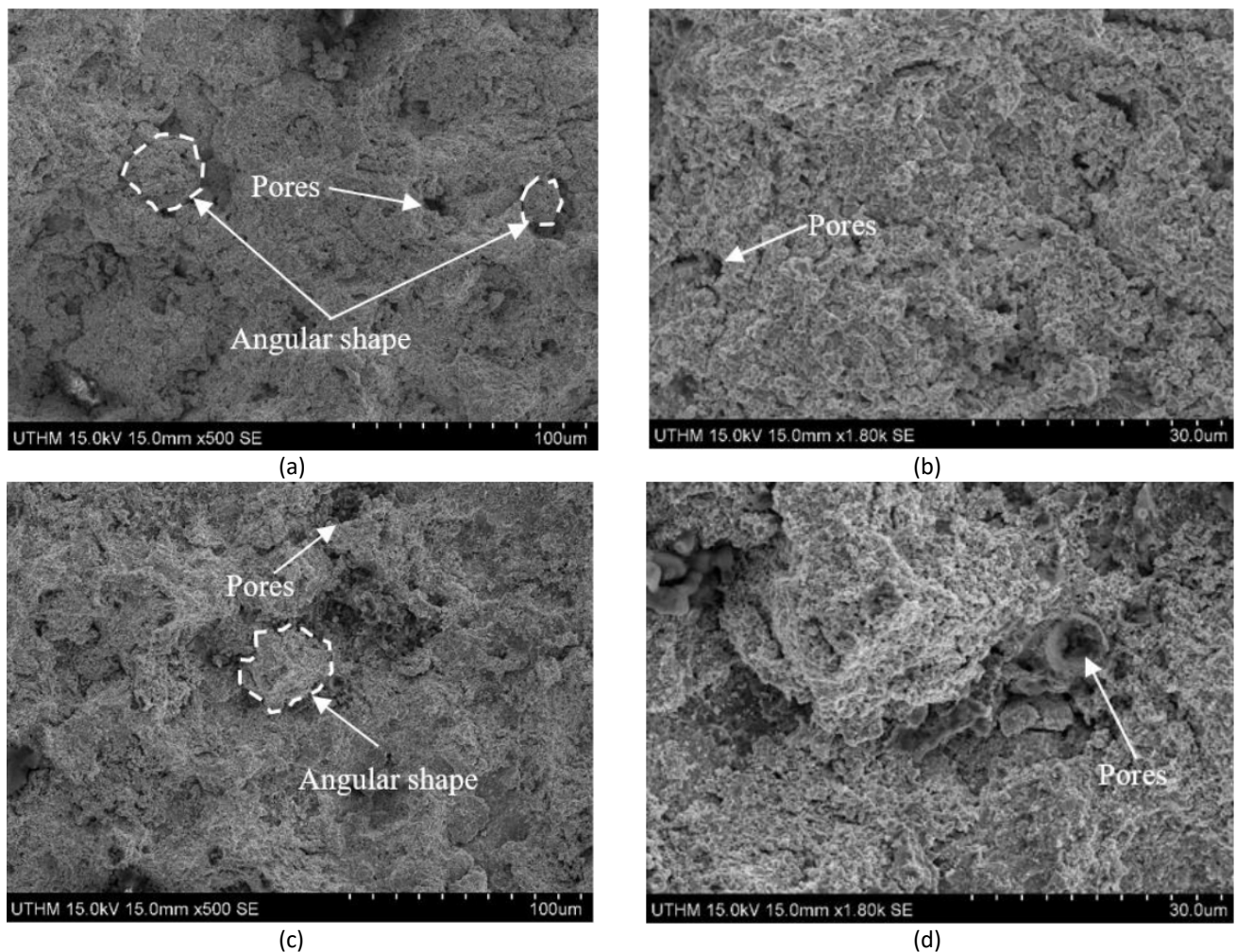


Fig. 2. SEM micrographs of WC-Ni coating; (a) low magnification (500x) and (b) high magnification (1800x) for 200 mm spraying distance, (c) low magnification (500x) and (d) high magnification (1800x) for 250 mm spraying distance

3.2 Fatigue Test Result

Based on the data presented in Table 3, it is evident that uncoated steel exhibits the highest fatigue strength among the tested materials. At a cycle count of 10^6 , the fatigue strength of uncoated steel is measured at 317 MPa. Following this, carbon steel coated with WC-Ni using a spraying distance of 250 mm demonstrates a fatigue strength of 250 MPa at the same cycle count. Lastly, carbon steel coated with WC-Ni using a spraying distance of 200 mm exhibits a fatigue strength of 250 MPa at 10^6 cycles. This trend is further supported by the corresponding lines shown in Figure 3. The line representing uncoated steel is positioned at the top, indicating its superior fatigue strength compared to the coated steel. Additionally, the line representing carbon steel coated with WC-Ni using a spraying distance of 250 mm is situated above the line representing carbon steel coated with WC-Ni using a spraying distance of 200 mm. This suggests that the former coating method yields higher fatigue strength. Moreover, the parallel alignment of all the lines in the graph indicates that no external factors, such as temperature variations or corrosion, significantly influenced the specimens during the testing process. This reinforces the results' reliability and suggests that the observed differences in fatigue strength can be attributed primarily to the effects of the coatings and spraying distances.

Table 3

The stress life (S-N) value for uncoated steel and WC-Ni coated carbon steel

Specimen	Coating Thickness (mm)	Spraying Distance (mm)	Load Amplitude, F_a (kN)	Fatigue Strength, σ_f (MPa)	Number of Cycles to failure, N_f
Uncoated	NA	NA	13.5	476	2365
			11.1	435	18908
			10.5	370	162151
			9.0	317	1000000
WC – Ni Coated Carbon Steel	0.25	200	13.3	480	135
			10.0	360	551
			8.4	305	197548
		250	6.9	250	1000000
			10.0	360	29070
			7.5	270	1000000

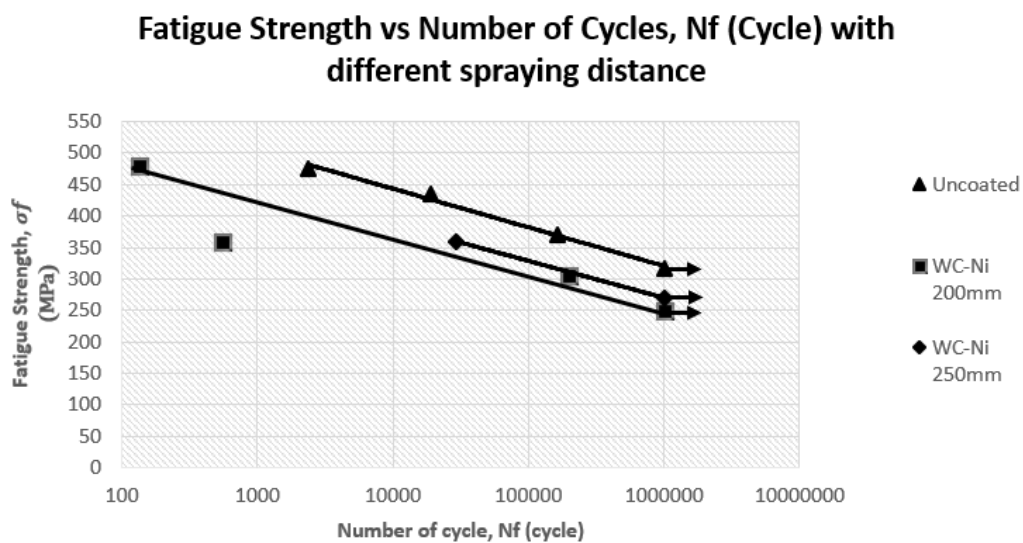


Fig. 3. The stress line (S-N) diagram of uncoated steel and WC-Ni coated steel

The fatigue strength of a material, expressed as a percentage of its ultimate tensile strength, can range significantly from 1% to 70%. Various factors, such as surface finish, specimen size, load type, temperature, corrosive environment, mean stresses, residual stresses, and stress concentrations influence this variability. For instance, high-strength steel with a sharp notch exposed to a high mean tensile stress in a corrosive environment typically demonstrates a fatigue strength of around 1% of its ultimate tensile strength. Conversely, medium-strength steel under an inert atmosphere with substantial compressive residual stress may exhibit a fatigue strength of approximately 70% of its ultimate tensile strength [18]. The relationship between fatigue strength and tensile strength is shown in Figure 4. The graph indicates a proportional increase in fatigue strength as tensile strength rises. However, the average fatigue ratio is approximately 0.33. Notably, this average value is lower than the expected value of 0.5. Table 4 shows the value of fatigue strength and tensile strength.

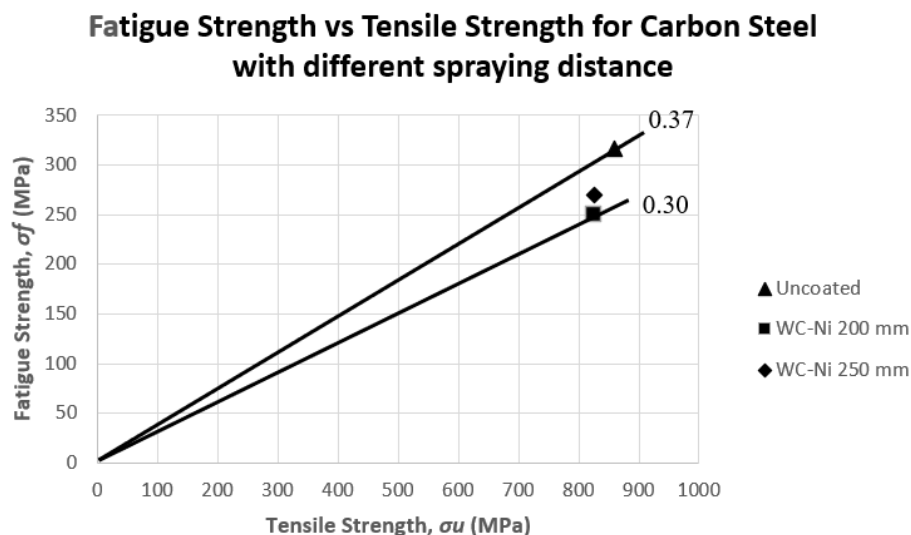


Fig. 4. The relation between fatigue strength and tensile strength

Table 4
 The fatigue strength and tensile strength value

	Tensile Strength, σ_u (MPa)	Fatigue Strength, σ_f (MPa)	Fatigue Ratio
Uncoated steel	858.4	317	0.37
WC-Ni 200 mm	825	270	0.33
WC-Ni 250 mm	825	250	0.30
Averaged value	836.1	279	0.33

3.3 Fracture Surface Observation

Figure 5 (a) shows the fractured surface of uncoated carbon steel with a fatigue strength of 317 MPa at the 10^6 cycles. Figure 5 (b) is the scanning electron microscope for the carbon steel specimen coated with WC-Ni with a 200 mm spraying distance. Meanwhile, Figure 5 (c) is the carbon steel coated with a 250 mm spraying distance of WC-Ni.

The fractured surface displays two distinct areas that can be observed: one is a burnished, smooth region, and the other is a granular, rough region. In Figure 5 (a), (b), and (c), the burnished, smooth region was designated as Region 1, while the granular, rough region was labelled as Region 2. The burnished, smooth region corresponds to the specific area where the fatigue crack occurred. Within this region, various features can be identified, including crack initiation sites, progression marks, a clamshell pattern, benchmark indicators, and striations. On the contrary, the granular, rough region represents the final ductile fracture area, which experienced a fracture relatively quickly compared to the fatigue crack region [19].

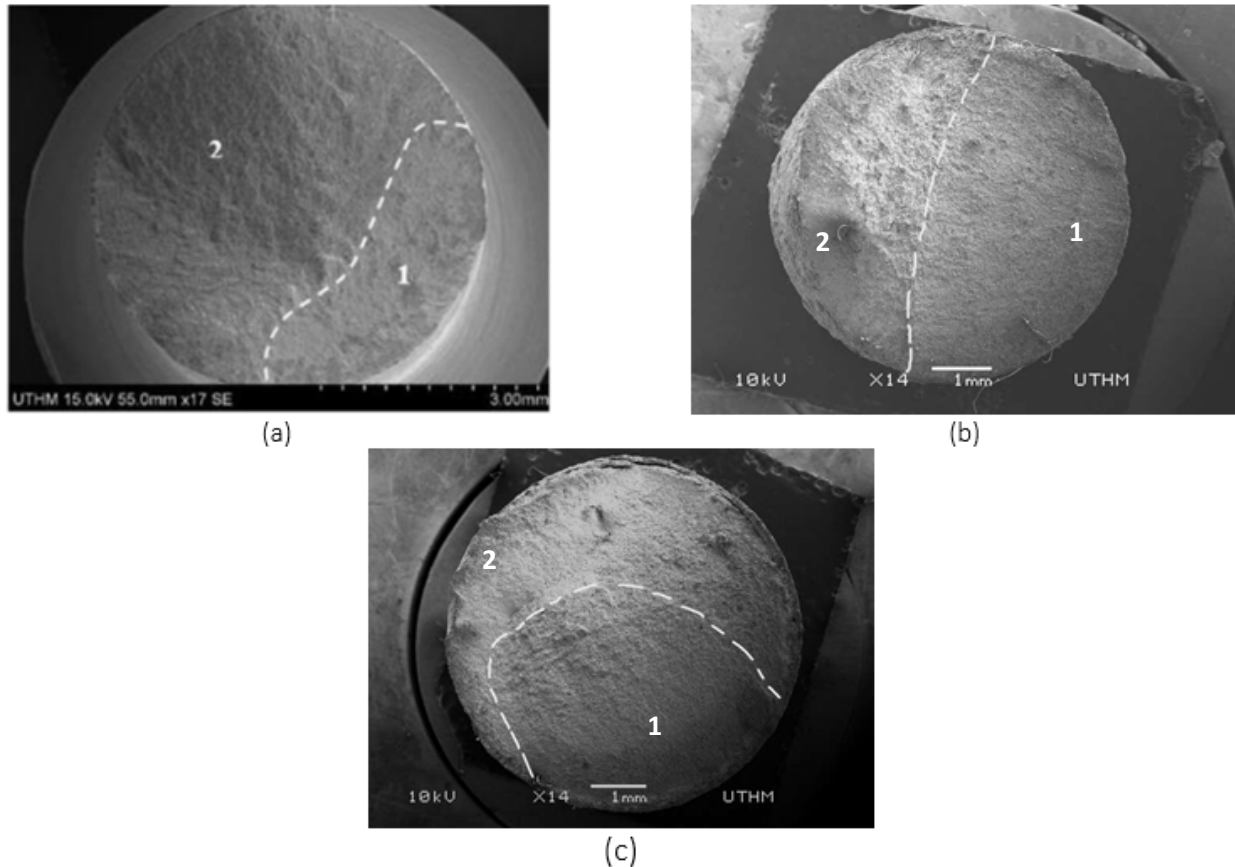


Fig. 5. (a) SEM micrograph of fractured surface for uncoated, (b) SEM micrograph for fractured surface for WC-Ni 200 mm spraying distance, (c) SEM micrograph of fractured surface for WC-Ni 250 mm spraying distance

According to Figure 6 (a), the fractured surface exhibits fatigue striations, which are tiny features that can be observed under microscopic examination. These striations indicate the fracture's advancement during each load cycle, revealing the gradual growth of a fatigue crack. However, it's important to distinguish fatigue striations from beach marks, which are macroscopic characteristics resulting from stress modifications that contribute to the progression of the crack tip. Unlike fatigue striations, beach marks provide a broader perspective and offer insights into the changing direction of fracture progression over time. Notably, a single beach mark can encompass a multitude of individual striations, potentially numbering in the thousands [20]. The visibility of these striations may be compromised due to extensive surface rubbing and pounding that occurs during repetitive loading. Additionally, it becomes exceedingly difficult to detect these striations in materials with high strength. Hence, the identification and examination of such striations pose significant challenges in such materials.

Based on Figure 6 (b), several initial cracks are observed near the upper right outer perimeter. These cracks are characterized by somewhat radial lines, commonly called "ratchet marks," which extend around the upper left perimeter. The process of initial cracking originated at the surface and subsequently propagated towards the interior of the specimen. According to G. A. Pantazopoulos [21], cracks tend to nucleate primarily at or near the surface due to several factors. Firstly, inelastic deformation is more likely to occur at the surface, making it a favourable location for crack initiation. Additionally, surface areas can experience intrusion or extrusion, resulting in increased stresses or strains from external loads. Manufacturing processes often lead to stress concentration at the surface, further contributing to crack nucleation. Moreover, surface-related factors such as

environmental attacks, such as corrosion, can promote crack initiation. However, it is important to note that cracks can also originate from non-surface areas, such as grain boundaries, inclusions, pores, and other microstructural features or discontinuities. These areas present potential sites for crack nucleation, indicating that cracks are not solely restricted to the surface region.

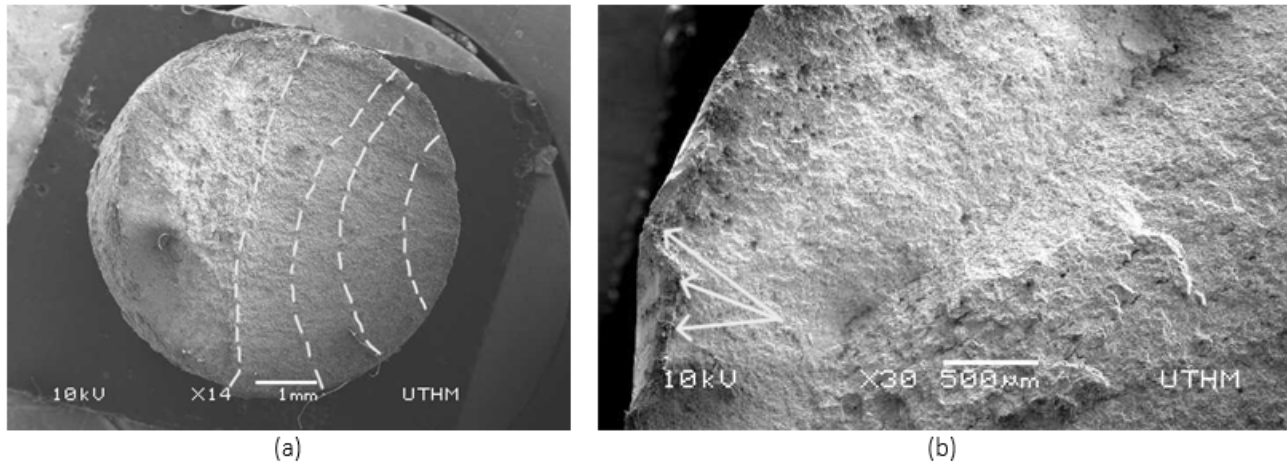


Fig. 6. (a) Fatigue striation at the fractured surface of 200 mm spraying distance of WC-Ni, (b) Fatigue initiation at the fractured surface of 250 mm WC-Ni coating of carbon steel

4. Conclusions

This study examines the impact of high-velocity tungsten carbide-nickel (WC-Ni) oxy-fuel coatings on the fatigue behaviour of carbon steel at various spray distances. The results showed that the fatigue tests demonstrated that carbon steel's fatigue strength decreased when coated using the HVOF method. The uncoated carbon steel exhibited the highest mechanical fatigue strength among all the tested samples. However, among the coated carbon steel samples, the WC-Ni coating applied at a spraying distance of 250 mm displayed the highest mechanical fatigue strength. This suggests that the fatigue strength of the coated carbon steel improves as the spraying distance increases. In other words, a greater spraying distance during the HVOF coating process enhances the fatigue strength of the carbon steel material. Nevertheless, a greater distance may sacrifice the porosity and mechanical properties of the coatings.

Acknowledgement

Communication of this research is made possible through monetary assistance by University Tun Hussein Onn Malaysia and the UTHM Publisher's Office via Publication Fund E15216.

References

- [1] Raza, Ali, Faiz Ahmad, Thar M. Badri, M. R. Raza, and Khurshid Malik. "An Influence of oxygen flow rate and spray distance on the porosity of HVOF coating and its effects on corrosion—A Review." *Materials* 15, no. 18 (2022): 6329. <https://doi.org/10.3390/ma15186329>
- [2] Prasad, C. Durga, Shanthala Kollur, C. R. Aprameya, T. V. Chandramouli, T. Jagadeesha, and B. N. Prashanth. "Investigations on tribological and microstructure characteristics of WC-12Co/FeNiCrMo composite coating by HVOF process." *JOM* 76, no. 1 (2024): 186-195. <https://doi.org/10.1007/s11837-023-06242-2>
- [3] Varis, T., Tomi Suhonen, Olof Calonius, J. Čuban, and M. Pietola. "Optimization of HVOF Cr3C2NiCr coating for increased fatigue performance." *Surface and Coatings Technology* 305 (2016): 123-131. <https://doi.org/10.1016/j.surfcoat.2016.08.012>
- [4] Nascimento, Marcelino P., Renato C. Souza, Ivancy M. Miguel, Walter L. Pigatin, and Herman JC Voorwald. "Effects of tungsten carbide thermal spray coating by HP/HVOF and hard chromium electroplating on AISI 4340 high

- strength steel." *Surface and coatings technology* 138, no. 2-3 (2001): 113-124. [https://doi.org/10.1016/S0257-8972\(00\)01148-8](https://doi.org/10.1016/S0257-8972(00)01148-8)
- [5] Hübler, Daniela, and Thomas Grad. "Effect of different binders and secondary carbides on NbC cermets." *Forschung im Ingenieurwesen* 86, no. 2 (2022): 197-211. <https://doi.org/10.1007/s10010-022-00583-1>
- [6] Taylor, S. R. "Coatings for Corrosion Protection: Metallic." *Encyclopedia of Materials: Science and Technology*. (2001): 1-5. <https://doi.org/10.1016/B0-08-043152-6/00239-4>
- [7] Kumar, Naveen, and Vikas Kumar Choubey. "Investigation of microstructure and Isothermal oxidation resistance of cermet HVOF coated on AISI316L at 900° C." *Results in Surfaces and Interfaces* 14 (2024): 100173. <https://doi.org/10.1016/j.rsurfi.2023.100173>
- [8] Baba, Nor Bahiyah, Amirul Syazwan Ghazali, Afifah Humaira Abdul Rahman, Nor Azinee Said, and Safian Sharif. "Influence of Heat Treatment on Microhardness and Surface Roughness of Electroless Ni-YSZ Composite Coating." *Journal of Advanced Research in Fluid Mechanics and Thermal Sciences* 99, no. 1 (2022): 114-122. <https://doi.org/10.37934/arfmts.99.1.114122>
- [9] Ganeev, Artur V., Marina V. Karavaeva, Xavier Sauvage, Eglantine Courtois-Manara, Yulia Ivanisenko, and Ruslan Z. Valiev. "On the nature of high-strength state of carbon steel produced by severe plastic deformation." In *IOP Conference Series: Materials Science and Engineering*, vol. 63, no. 1, p. 012128. IOP Publishing, 2014. <https://doi.org/10.1088/1757-899X/63/1/012128>
- [10] Itoh, Takamoto, Fumio Ogawa, and Takahiro Morishita. "Fatigue Testing and Evaluation of Fatigue Strength under Multiaxial Stress State; Why do we need fatigue testing?." In *MATEC Web of Conferences*, vol. 159, p. 01050. EDP Sciences, 2018. <https://doi.org/10.1051/mateconf/201815901050>
- [11] Halmi, M. A. M., Harimon, M. A., Ismail, A. E., and Chue, D., "Fatigue behaviour of high velocity oxy-fuel coatings on medium carbon steel," *Int. J. Eng. Trends Technol.*, vol. 69, no. 6 (2021): 56–70. <https://doi.org/10.14445/22315381/IJETT-V69I6P209>
- [12] Scendo, M. and Staszewska-Samson, K. "Effect of Standoff Distance on Corrosion Resistance of Cold Sprayed Titanium Coatings." *Coatings*. no.12 (2022): 1853. <https://doi.org/10.3390/coatings12121853>
- [13] Wang, Wei-Ze, Chang-Jiu Li, and Yu-Yue Wang. "Effect of spray distance on the mechanical properties of plasma sprayed Ni-45Cr coatings." *Materials transactions* 47, no. 7 (2006): 1643-1648. <https://doi.org/10.2320/matertrans.47.1643>
- [14] La Barbera-Sosa, J. G., Y. Y. Santana, C. Villalobos-Gutiérrez, S. Cabello-Sequera, M. H. Staia, and E. S. Puchi-Cabrera. "Effect of spray distance on the corrosion-fatigue behavior of a medium-carbon steel coated with a Colmonoy 88 alloy deposited by HVOF thermal spray." *Surface and Coatings Technology* 205, no. 4 (2010): 1137-1144. <https://doi.org/10.1016/j.surfcoat.2010.01.038>
- [15] Rajendran, Pradeep Raj, Thirumalaikumarasamy Duraisamy, Ramachandran Chidambaram Seshadri, Ashokkumar Mohankumar, Sathiyamoorthy Ranganathan, Guruprasad Balachandran, Kaliyamoorthy Murugan, and Laxmi Renjith. "Optimisation of HVOF spray process parameters to achieve minimum porosity and maximum hardness in WC-10Ni-5Cr coatings." *Coatings* 12, no. 3 (2022): 339. <https://doi.org/10.3390/coatings12030339>
- [16] ASTM Standard E466. Conducting Force Controlled Constant Amplitude Axial Fatigue Tests of Metallic Materials. West Conshohocken: ASTM International, (2015).
- [17] Zou, Yong-Ming, Yao-Sha Wu, Ji-Zhong Wang, Z. G. Qiu, and D. C. Zeng. "Preparation, mechanical properties and cyclic oxidation behavior of the nanostructured NiCrCoAlY-TiB₂ coating." *Ceramics International* 44, no. 16 (2018): 19362-19369. <https://doi.org/10.1016/j.ceramint.2018.07.165>
- [18] Stephens, Ralph I., Ali Fatemi, Robert R. Stephens, and Henry O. Fuchs. *Metal fatigue in engineering*. John Wiley & Sons, 2000.
- [19] Siegl, J., Nedbal, I., and Kunz, J. "Fractographic study of fatigue processes, in *Fracture Damage of Structural Parts*", (2004): 165–172.
- [20] Hertzberg, Richard W., Richard P. Vinci, and Jason L. Hertzberg. *Deformation and fracture mechanics of engineering materials*. John Wiley & Sons, 2020.
- [21] Pantazopoulos, George A. "A short review on fracture mechanisms of mechanical components operated under industrial process conditions: Fractographic analysis and selected prevention strategies." *Metals* 9, no. 2 (2019): 148. <https://doi.org/10.3390/met9020148>